Acknowledgements

References

[1] Baughman RH, Zakhidov AA, de Heer WA. Carbon nanotubes – the route toward applications. Science 2002;297:787–92.

[2] Barber AH, Cohen SR, Wagner HD. Measurement of carbon nanotube–polymer interfacial strength. Appl Phys Lett 2003;82:4140–2.

[3] Bhattacharrya AR, Sreekumar TV, Liu T, Kumar S, Ericson LM, Hauge RH, et al. Crystallization and orientation studies in polypropylene/single wall carbon nanotube composite. Polymer 2003;44:2373–7.

[4] Sreekumar TV, Liu T, Min BG, Guo H, Kumar S, Hauge RH, et al. SWNT/PAN composite fibers. Adv Mater 2004;16:58–61.

[5] Zhang X, Liu T, Sreekumar TV, Kumar S, Hu X, Smith K. Gel spinning of PVA/SWNT fibers. Polymer 2004;45:8801–7.

[6] Qian D, Liu WK, Ruoff RS. Load transfer mechanism in carbon nanotube ropes. Compos Sci Technol 2003;63:1561–9.

[7] Didenko VV, Moore VC, Baskin DS, Smalley RE. Single-walled carbon nanotubes by fluorescent polymer wrapping. Nano Lett 2005;5:1563–7.

[8] Zhang X, Sreekumar TV, Liu T, Kumar S. Properties and structure of nitric acid oxidized single wall carbon nanotube films. J Phys Chem B 2004;108:16435–40.

[9] Dyke CA, Tour JM. Unbundled and highly functionalized carbon nanotubes from aqueous reactions. Nano Lett 2003;3:1215–8.

[10] Park C, Ounaies Z, Watson KA, Crooks RE, Smith Jr, Lowther SE, et al. Dispersion of single wall carbon nanotubes by in-situ polymerization under sonication. Chem Phys Lett 2002;364:303–8.

[11] Bajaj P, Sreekumar TV, Sen K. Production of high tenacity acrylic fibres. Chem Fibre Intern 1998;48:308–15.

[12] Bajaj P, Sreekumar TV, Sen K. Thermal behaviour of acrylonitrile copolymers having methacrylic and itaconic acid comonomers. Polymer 2001;42:1707–18.

[13] Min BG, Sreekumar TV, Uchida T, Kumar S. Oxidative stabilization of PAN/SWNT composite fibers. Carbon 2005;43:599–604.

[14] Chae HG, Minus ML, Kumar S. Oriented and exfoliated single wall carbon nanotubes in polyacrylonitrile. Polymer 2006;47:3494–504.

Raman scattering from an individual tubular graphite cone

P.H. Tan [a,*], J. Zhang [a], X.C. Wang [a], G.Y. Zhang [b], E.G. Wang [b]

[a] *State Key Laboratory for Superlattices and Microstructures, Institute of Semiconductors, Chinese Academy of Sciences, Beijing 100083, China*
[b] *State Key Laboratory for Surface Physics, Institute of Physics, Chinese Academy of Sciences, Beijing 100080, China*

Carbon has the wide variety of forms, such as diamond, graphite, fullerenes and nanotubes. These materials play an important role in the applications of field emission displays, transistors, hydrogen storage, etc. [1]. This causes that the studies on the carbon-based materials are one of the most active research fields of physical and chemical sciences continuously. During past few years, some non-planar graphitic structures have also been synthesized or found in nature, which include graphite polyhedral crystals, carbon cones and graphitic whiskers [2–5]. To identify and characterize these materials using many available experimental methods, is a key part of the research work of the optimization of these materials for applications. Raman microscopy, as a non-destructive and fast tool with high resolution, is widely applied for the characterization of various carbon materials [6,7]. Recently, the so-called tubular graphite cones (TGCs) are synthesized on an iron needle using a chemical vapor deposition method [5]. One of potential applications for TGCs is for use as tips of scanning probe microscopy because of the greater rigidity and easier mounting than currently used carbon nanotubes. In this letter, we report the results of the Raman spectroscopy studies on an individual tubular graphite cone.

The tubular graphite cones have nanometer-sized tips, micrometer-sized roots and hollow interiors with a diameter ranging from about two to several tens of nanometers. The cones are composed of cylindrical graphite sheets; a continuous shortening of the graphite layers from the interior to the exterior makes them cone-shaped. All of the tubular graphite cones have a faceted morphology. Their detail structural properties and scanning electron microscope, transmission electron microscope (TEM) and electron diffraction patterns had been described elsewhere [5]. The size of the diameter and length of the TGCs grown on iron needles are large enough to be seen from the camera of Raman system. The insets in Fig. 1 show optical images of the measured iron needle, where an individual TGC can be clearly identified and easily relocated. Many graphite microcrystals (GMs) were also found on the surface of iron needles, whose optical micro-images are shown in the right inset of Fig. 1.

The Raman spectra were recorded by the Dilor Super Labram with a typical resolution of 0.5–2 cm^{-1} in a back-

---
[*] Corresponding author. Fax: +44 1223 748348.
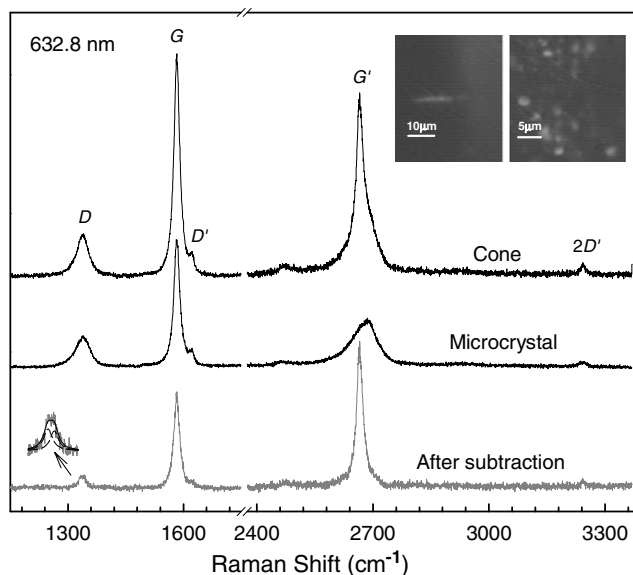*E-mail address:* pt290@eng.cam.ac.uk (P.H. Tan).

Fig. 1. Raman scattering of the tubular graphite cone and graphite microcrystal in the as-grown sample excited by a 632.8-nm laser. The insets show the optical micro-images of the tubular graphite cone and graphite microcrystals. The gray line shows the spectrum of the tubular graphite cone subtracted from that of the graphite microcrystal.
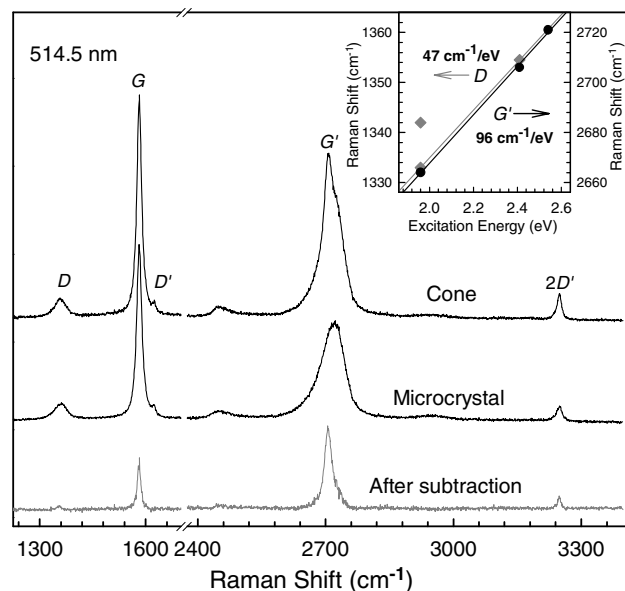

Fig. 2. Raman scattering of the tubular graphite cone and graphite microcrystal excited by a 514.5-nm laser. The gray line shows the spectrum of the tubular graphite cone subtracted from that of the graphite microcrystal and its energy dispersion of the D and G′ modes is shown in the inset.

scattering geometry at room temperature. The system consists of holographic notch filters for Rayleigh rejection and a microscope with 50× objective lens, allowing a spatial resolution of ∼1.0 μm. The laser excitation wavelengths are 514.5 nm, 488.0 nm of an Ar$^+$ laser and 632.8 nm of a He–Ne laser. Typically, a low laser power of 0.1 mW arrived at the sample was used to avoid sample heating.

Raman scatterings from the individual TGC and a graphite microcrystal excited by a 632.8-nm laser are shown in Fig. 1. Their Raman spectra exhibit a typical spectral feature of graphite materials. The Raman peaks at about 1340, 1580 and 1620 cm^{-1} are the first-order Raman modes and be usually called as the D, G and D′ modes, and the Raman peaks at about 2660 and 3240 cm^{-1} are the overtones of the D and D′ modes [8], respectively. The G mode is a $\vec{k} = 0$ zone-center optical mode in graphite materials, and the D and D′ modes are not zone-center optical modes ($\vec{k} \neq 0$), which become Raman active due to the double resonance Raman scattering process [9–11]. The linewidth of the G mode in the TGC and GM is slightly larger than that of highly oriented pyrolytic graphite (HOPG). The intensity of the D mode relative to that of the G mode is also weak in the TGC and graphite microcrystal. All of those indicate that TGCs and GMs have a high crystal quality, which agrees with the results from scanning electron microscope and electron diffraction patterns studies [5].

The Raman spectrum of the GM is similar to that of ion-implanted HOPG under the same excitation [8], such as a broad spectral structure of the G′ mode and a lower intensity of the G′ mode relative to the G mode. However, the Raman spectrum of the TGC shows an asymmetric line

shape of a G′ mode where a sharp peak is located at about 2665 cm^{-1} along with two shoulders at its high- and low-energy sides. This feature is different from the peak profile of the G′ mode of other graphite materials [3,12,13]. Except the sharp peak at 2665 cm^{-1}, the other part of the G′ mode in the TGC is, however, very similar to that of the broad G′ peak of the GM. The Raman spectrum of the TGC subtracted from that of the GM is shown as the gray line in Fig. 1, in which the sharp G′ peak at 2665 cm^{-1} exceeds in intensity the corresponding G band, as the case in graphite whiskers and graphite polyhedral crystals [3,12]. The Lorentzian line shape is used to fit the spectrum of the gray line in Fig. 1, and the fitted linewidths of the D, G, G′ and 2D′ modes in the remnant spectrum are 18, 18, 20 and 9 cm^{-1}, respectively, which is very close to those in graphite whiskers [12]. The peak position of the G (1582 cm^{-1}) and G′ (2665 cm^{-1}) modes are also almost equal to those in graphite whiskers.

To further confirm that the sharp peak of G′ mode at 2665 cm^{-1} in Fig. 1 is one intrinsic mode of the tubular graphite cone, 488.0-nm and 514.5-nm lasers are used to excited the Raman spectra of the tubular graphite cone and Raman spectra excited by a 514.5-nm laser are shown in Fig. 2. Similar results are observed for the two excitations, and the G′ mode in the TGC also shows an asymmetric line shape with a sharp peak at about 2706 cm^{-1} for 514.5-nm excitation. After subtracted from the Raman spectrum of the GM, the remnant spectrum of the TGC exhibits a whisker-like spectral feature again. The intensity of the D mode in the remnant spectrum is much weak under the short-wavelength excitation and only one weak peak at 1354 cm^{-1} can be resolved for the 514.5-nm

excitation. Moreover, this peak is too weak to be identified the 488.0-nm excitation. It is a typical D mode behavior of Raman spectra from graphite materials [13].

The studied TGC has a length of 15 μm and is horizontally accreted at the left side of an iron needle as shown in Fig. 1. According to the size of the TGC and the spot size (∼1 μm) of the excitation laser, it is expected that all Raman signals are from the measured individual TGC, but not GM and other nanostructured carbons. The observed results in Figs. 1 and 2 reveal that the two-phase spectral feature of the intrinsic Raman signal of the TGC is composed of two parts: one is similar to the spectrum of the GM (called GM-like part for short) and the other is similar to that of graphite whiskers [12] (called whisker-like part for short).

The high-resolution TEM image shows that TGCs and GMs have a well-ordered graphitic structure with an inner interlayer spacing of ∼0.34 nm. The GM-like part of the Raman signal of the TGC, therefore, originates from the inner graphite layers of the TGC with a well-ordered graphitic structure. Different from the solid-state graphitization of amorphous carbon, the gas-phase grown graphite whiskers, carbon cones and other filamentous graphite usually have a well-defined curved termination of graphite sheets to eliminate all of the dangling bonds [2–4]. The formation of semicylindrically bent graphitic layers makes the termination of the graphite sheets in the surface and brim regions look like multiple-walled nanotube tips in the cross-section [3,4,12]. In those materials, the intensity enhancement of the G′ mode relative to the G mode are observed, but no enhancement observed for the common graphite materials. The whisker-like spectral features in gray lines of Figs. 1 and 2 suggest that TGCs may exhibit a similar termination of frill-like bent graphitic layers as the case of graphite whisker and graphite polyhedral crystals [3,12], and the whisker-like part of Raman signal in the TGC is favorably from the surface layers of the TGC with such structures. In graphite whisker, the intensity of the G′ overtone is found to be about 13 times stronger than that of the G mode [12]. Because the average tip apex angle of the TGC is 6–7°, the number of the frill-like bent graphite layers in the surface of the TGC are much less than that in the surface of graphite whiskers, and thus the intensity enhancement of the G′ mode to the G mode in the TGC is expected much weaker than that in graphite whiskers.

The inset of Fig. 2 shows the dependence of the D and G′ modes of the whisker-like component of Raman spectra from the TGC on the laser excitation energy. For the 632.8-nm laser excitation, the D mode in the remnant spectrum of the gray line can be well fitted by two peaks at about 1332 and $1342 \, cm^{-1}$ and the frequency of the G′ mode is just two times that of the low-energy D mode at $1332 \, cm^{-1}$. The doublet structure of the D mode had been clearly observed in graphite whiskers, which results from the double resonant Raman process of the first-order dispersive modes in carbon materials [11,14]. If only considering the low-energy peak of the D mode, the frequency shift

of the D and G′ modes with excitation energy are with a slope of 47 and $96 \, cm^{-1}/eV$ as shown in the inset of Fig. 2, which are very close to that of the D and G′ modes in graphite whiskers [12]. This also confirms that the whisker-like spectrum of gray lines in Figs. 1 and 2 are the intrinsic Raman signal from the studied TGC.

The studies on the graphitic foams show that the peak position and dispersion of the G′ mode are closely related to graphitic structures, which is three-dimensional (3D) one with well-stacked planes or two-dimensional (2D) one with weak interaction between unaligned graphene layers [15]. The asymmetrical spectral profile of the G′ mode of GMs indicates that GMs exhibit a 3D graphitic structure. However, frill-like bent graphite layers in the surface of TGCs and graphite whiskers have a turbostratic graphitic structure. Such a structure make the Raman spectra from the surface regions of TGCs and graphite whiskers resemble that of the typical 2D graphite, for an example, the frequency of the whisker-like G′ mode in the TGC downshifts about $22–24 \, cm^{-1}$ with respect to that in HOPG [8], a 3D graphite, and its dispersion ($96 \, cm^{-1}/eV$) is close to that ($99 \, cm^{-1}/eV$) of 2D graphite [15]. The curvature of frill-like graphite layers near the surface region could result in an additional frequency shift of the G′ mode, but this curvature can also lead to the frequency shift of the G mode. However, relative to the G mode in GMs, we do not observe any shift of the whisker-like G mode in the TGC as shown by gray lines in Figs. 1 and 2. Also, the frequency and dispersion of the whisker-like G′ mode in the TGC is exactly the values of linear interpolation between those of the G′(2D) and G′(3D) peaks observed in graphitic foams [15]. Therefore, the frequency position of the whisker-like G′ mode in TGCs does not result from the curvature effect [16] of frill-like graphite layers near the surface region, but directly from the 2D and 3D arrangements of the graphene layers.

The above results show that Raman scattering can be used to distinguish the different graphite structures between the outer graphite layers near the surface and the inner graphite layers in TGCs. The outer graphite layers near the surface of TGCs are formed with the frill-like bent graphite layers, which makes the corresponding Raman spectrum be similar to that of the typical 2D turbostratic graphite. However, the inner graphite layers in TGCs are well ordered [5] and their Raman spectra assemble that of the 3D graphite. It should be pointed out that most of tubular graphite cones on iron needle exhibits two-phase Raman spectral behavior, and only a few of them not. The intensity of the whisker-like part of Raman spectra also varies with different measured TGCs. This is mainly due to the too complex growth process of carbon filaments in chemical vapor deposition to control the frill-like bent structures of graphite layers at the surface of TGCs [5]. The frill-like bent graphite layers in the brim region of TGCs revealed from Raman spectrum may be one of the main reasons to keep one TGC with identical zigzag chiralities.

In summary, Raman scattering is applied to characterize tubular graphite cones and graphite microcrystals synthesized on an iron needle using the chemical vapor deposition method. Tubular graphite cones and graphite microcrystals are shown to have a high crystal quality. The G′ Raman peak of tubular graphite cones shows an asymmetric line shape, and is composed of two parts: one is similar to Raman spectrum of graphite microcrystals with a well-ordered 3D graphitic structure, and the other is similar to that of graphite whiskers, which is from the 2D graphitic structure with frill-like bent graphite layers near the surface regions of tubular graphite cones. The measured excitation-energy dependence of 47 and 96 cm^{-1}/eV, respectively, for the D and G′ modes of the whisker-like Raman signal in tubular graphite cones is very close to that in graphite whiskers, which further confirms the above results. Again, Raman spectroscopy is shown here be an essential characterization tool for the study of the structure information of 2D and 3D arrangements of the graphene layers.

Acknowledgements

References

[1] Dresselhaus MS, Dresselhaus G, Eklund PC. Science of fullerenes and carbon nanotubes. New York: Academic Press; 1998.

[2] Bacon R. Growth, structure, and properties of graphite whiskers. J Appl Phys 1960;31(2):283–90.

[3] Gogotsi Y, Libera JA, Kalashnikov N, Yoshimura M. Graphite polyhedral crystals. Science 2000;290(5490):317–20.

[4] Dong J, Shen WC, Zhang BF, Liu X, Kang FY, Gu JL, et al. New origin of spirals and new growth process of carbon whiskers. Carbon 2001;39(15):2325–33.

[5] Zhang GY, Jiang X, Wang EG. Tubular graphite cones. Science 2003;300(5618):472–4.

[6] Eklund PC, Holden JM, Jishi RA. Vibrational modes of carbon nanotubes; spectroscopy and theory. Carbon 1995;33(7):959–72.

[7] Ferrari AC, Robertson J, editors. Raman spectroscopy in carbons: from nanotubes to diamond. London: Royal Society; 2004.

[8] Tan PH, Deng YM, Zhao Q. Temperature-dependent Raman spectra and anomalous Raman phenomenon of highly oriented pyrolytic graphite. Phys Rev B 1998;58(9):5435–9.

[9] Thomsen C, Reich S. Double resonant Raman scattering in graphite. Phys Rev Lett 2000;85(24):5214–7.

[10] Saito R, Jorio A, Souza Filho AG, Dresselhaus G, Dresselhaus MS, Pimenta MA. Probing phonon dispersion relations of graphite by double resonance Raman scattering. Phys Rev Lett 2002;88(2):027401.

[11] Tan PH, An L, Liu LQ, Guo ZX, Czerw R, Carroll DL, et al. Probing the phonon dispersion relations of graphite from the double-resonance process of Stokes and anti-Stokes Raman scatterings in multiwalled carbon nanotubes. Phys Rev B 2002;66(24):245410.

[12] Tan PH, Hu CY, Dong J, Shen WC, Zhang BF. Polarization properties, high-order Raman spectra, and frequency asymmetry between Stokes and anti-Stokes scattering of Raman modes in a graphite whisker. Phys Rev B 2001;64(21):214301.

[13] Reich S, Thomsen C, Maultzsch J. Carbon nanotubes. Berlin: Wiley-VCH; 2004.

[14] Cançado LG, Pimenta MA, Saito R, Jorio A, Ladeira LO, Grünis A, et al. Stokes and antiStokes double resonance Raman scattering in two dimensional graphite. Phys Rev B 2002;66(03):035415.

[15] Barros EB, Demir NS, Souza Filho AG, Mendes Filho J, Jorio A, Dresselhaus G, Dresselhaus MS. Raman spectroscopy of graphitic foams. Phys Rev B 2005;71(16):165422.

[16] Souza Filho AG, Jorio A, Samsonidze GG, Dresselhaus G, Pimenta MA, Dresselhaus MS, et al. Competing spring constant versus double resonance effects on the properties of dispersive modes in isolated single-wall carbon nanotubes. Phys Rev B 2003;67(03):035427.

Growth of CNTs on hydrogen plasma etched Fe–Si thin films

Jyh-Ming Ting *, Shih-Wei Hung

Department of Materials Science and Engineering, National Cheng Kung University, Tainan, Taiwan

Catalysts for the growth of carbon nanotubes (CNTs) can be a single element catalyst or contain more than one element. An elemental catalyst, such as Ni or Mo, generally allows the growth of CNTs through a multi-step process to form CNTs [1,2]. To improve the performance of elemental catalysts, an additive such as Mo or Y may be used [3,4]. The second minor element has been found to, for example, lower the CNT growth temperature [5] or prevent the formation of undesired graphite particles [6]. We have also reported previously a high-rate growth (13 μm/min) of aligned CNTs at a temperature of 370 achieved by adding Si to a Fe thin film catalyst [7,8]. The CNTs were found to

* Corresponding author. Fax: +886 6 238 5613.
  E-mail address: jting@mail.ncku.edu.tw (J.-M. Ting).